

## **General Disclaimer**

### **One or more of the Following Statements may affect this Document**

- This document has been reproduced from the best copy furnished by the organizational source. It is being released in the interest of making available as much information as possible.
- This document may contain data, which exceeds the sheet parameters. It was furnished in this condition by the organizational source and is the best copy available.
- This document may contain tone-on-tone or color graphs, charts and/or pictures, which have been reproduced in black and white.
- This document is paginated as submitted by the original source.
- Portions of this document are not fully legible due to the historical nature of some of the material. However, it is the best reproduction available from the original submission.

**NASA Technical Memorandum 79192**

**(NASA-TM-79192) SOME FLOW CHARACTERISTICS  
OF CONVENTIONAL AND TAPERED HIGH PRESSURE  
DROP SIMULATED SEALS (NASA) 18 p  
HC A02/MF A01**

**N79-27460**

**CSCL 20D**

**Unclas  
G3/34 29274**

**SOME FLOW CHARACTERISTICS OF  
CONVENTIONAL AND TAPERED HIGH  
PRESSURE DROP SIMULATED SEALS**

**R. C. Hendricks  
Lewis Research Center  
Cleveland, Ohio**

**Prepared for the  
Joint Lubrication Conference  
cosponsored by the American Society of Lubrication Engineers  
and the American Society of Mechanical Engineers  
Dayton, Ohio, October 16-18, 1979**

SOME FLOW CHARACTERISTICS OF CONVENTIONAL AND  
TAPERED HIGH PRESSURE DROP SIMULATED SEALS

by R. C. Hendricks

National Aeronautics and Space Administration  
Lewis Research Center  
Cleveland, Ohio 44135

ABSTRACT

The leak rates through shaft seals with large pressure drops were simulated using gaseous hydrogen, or nitrogen flowing through an annulus with a nonrotating centerbody. The flows were choked. For concentric or eccentric position of the rotor and parallel or convergent tapered flow passages, data and analysis revealed that mass flux or leak rate can be determined from a relation whose normalizing parameters depend on the thermodynamic critical constants of the working fluid and an average flow area expressed in terms of the inlet and exit cross-sectional areas. Using these normalized relations, the flow data for parallel and three convergent tapered shaft seal configurations are in good agreement. Generalization to any simple gas or gas mixture is implied and demonstrated in part.

NOMENCLATURE

A	flow area, $\text{cm}^2$
$\bar{A}$	average flow area, $\text{cm}^2$
C	normalization constant
D	diameter, cm
G	mass flux, $\text{g}/\text{cm}^2\text{-s}$
$G^*$	flow normalizing constant, $\sqrt{P_c \rho_c / Z_c}$ , $\text{g}/\text{cm}^2\text{-s}$
$G_R$	reduced mass flow, $G/G^*$
h	clearance height, cm
L	length, cm
m, n	exponents
P	pressure, MPa
$P_R$	reduced pressure, $P/P_c$
$R_0$	rotor radius, cm
T	temperature, K
$T_R$	reduced temperature, $T/T_c$
Z	compressibility

$\rho$  density, g/cm<sup>3</sup>  
 $\dot{m}$  mass flow rate, g/s

Subscripts:

c thermodynamic critical  
 e exit or exhaust  
 I inlet  
 t throat  
 0 stagnation

### INTRODUCTION

A well known rule of thumb in industrial practice is to provide some convergence in the design of seal flow passages to minimize the possibility of negative stiffness. The "rule" has not been established qualitatively or quantitatively, however Fleming (1) has found increased stiffness in his analysis of convergent flow passages with an optimum occurring at an inlet to exit clearance ratio of about 1.8. Often overlooked or minimized by large L/D are the effects of the inlet. References 2 to 4 demonstrate that in some cases, inlet geometry can be of significance in establishing flow rates and pressure profiles. Well instrumented 90° sharp edge and Borda type inlet results to 105 L/D not only indicate flow separation near the inlet, but in some cases of sufficient strength to be classified as critical flow at the inlet. For gases the flow recovery to 0.8  $P_0$  was common where  $P_0$  is the stagnation pressure.

In many seal designs, the pressure drop across the sealing surface is only large enough to choke the flow and some seals are not choked at all; however, many current designs require stagnation pressures many times the necessary "2:1" for choking. Little data are available on flows through seals with large axial pressure gradients with both concentric and eccentric positioning of the rotor in the housing including the effects of convergent conical tapers.

Thus the purpose of these tests will be to determine the mass flux through a simulated seal configuration with the fixed "rotor" held in both the concentric and fully eccentric positions.

## APPARATUS AND INSTRUMENTATION

The basic flow facility was of the blowdown type and is described in detail in Ref. 5. The system was modified somewhat to accommodate the housing which simulated the seal configuration from the space shuttle main fuel pump interstage seal. A schematic of the modified facility is given as Fig. 1. Although the system can handle cryogenics as well, the primary objective of these tests is to determine the flow rates for gases nitrogen or hydrogen, with and without back-pressure. The system back-pressure was controlled by injecting gaseous nitrogen into the exhaust cone. Figure 2 is a photograph of the seal assembly installed in the facility. A cross-section of the seal assembly is shown as Fig. 3. The conical adaptor flanges on each end, while not a part of the seal configuration, are necessary to provide proper flow distribution and measure temperature and pressure. For these tests, the seal housing was modified while the centerbody simulating the rotor, remained unaltered. A photograph of the instrumented centerbody and the housing prior to modifications is shown as Fig. 4. Previous experience indicated that minor misalignment could readily be detected in the pressure profiles and in the eccentric position, the nonuniform force distribution could be large; so in order to minimize misalignment and movement, four tabs at the inlet and outlet were used to hold the simulated rotor (centerbody) in a fixed position, see Fig. 5. The configurations were machined and data taken in such a way that two basic housings could provide all the necessary geometric changes. One was machined to give concentric alignment and the other fully eccentric positioning (i.e., contact simulation). Also shown in Fig. 5 are the pressure taps whose locations are given in Table 1 along with geometric parameters for the simulated rotor and housing. It is difficult to see the tapers, yet the flow rates are significantly affected.

The flow rates were metered using a venturi flowmeter located in the bottom of the storage tank and checked against an orifice flowmeter when appropriate, that is, when back-pressure control gas was not used. Inlet stagnation conditions were measured in a mixing chamber, not readily visible in Fig. 2, and for data reduction the average of four pressures within the seal ( $P_{02,5,6,9}$ ) was used.

## THEORETICAL BACKGROUND

Within a flow passage as shown in Fig. 5, usually one dimensional flow provides an adequate description. Extending some work on two phase choked flows and applying the principle of corresponding states (6-10) one can establish choked flow parameters over a large range in temperature, pressure, and working fluids.

The normalizing parameters (6-10) are  $G^*$ ,  $T_c$ ,  $P_c$  where

$$G^* = \sqrt{\frac{P_c \rho_c}{Z_c}} \quad (1)$$

and  $P_c$ ,  $T_c$ ,  $\rho_c$ ,  $Z_c$  are the pressure, temperature, density and compressibility of the working fluid at its thermodynamic critical point. See Table 2 for values of the critical constants for nitrogen, hydrogen, oxygen, argon, and methane. Further, it was determined that the choked flow of real gases could be represented over a large range in pressure and temperature by

$$\frac{G_R T_{R0}^n}{P_{R0}^m} = C \quad (2)$$

where  $G_R = G/G^*$ ,  $T_{R0} = T_0/T_c$ ,  $P_{R0} = P_0/P_c$ ,  $0.5 < n < 0.55$  and  $1. < m < 1.02$ . A similar form was advocated by Shapiro (11) for air. Equilibrium nozzle computations using fluids nitrogen, hydrogen, oxygen, argon, and methane were carried out using the methods of Refs. 6 to 9 the most appropriate value of the constant appears to be

$$C = \frac{1}{5} \quad (3)$$

for  $n = 0.5$  and  $m = 1.$ , with a scatter for fluid nitrogen of about 5 percent. With  $n = 0.55$  the scatter is decreased to about 1 percent with the constant increased to about 0.213. There also appears to be a trend with reduced pressure such that  $m = 1.02$ ; however for the extensive characterization of hydrogen,  $m = 1.0$ . Such trends indicate that for a given range of conditions and a given fluid, some improvement over Eq. (3) can be found.

Recalling that sharp edge inlets in some cases represent a real flow loss of  $0.2 P_0$ , it should follow that experimental flows should be less than 80

percent of the predicted nozzle flows; that is, in Eq. (2), for  $n = 0.5$ ,  $m = 1.0$ , the constant should be about 0.16.

For tapered geometries, the proper normalizing area for mass flux ( $G = \dot{m}/\bar{A}$ ) was estimated from some experience to be

$$\bar{A} = \frac{2A_e + A_I}{3} \quad (4)$$

where  $A_e$  is the exhaust flow area and  $A_I$  the entrance flow area. The calculated average area was found to be

$$3\bar{A} = A_e + A_I + \pi(R_0 + h_e)(R_0 + h_I) - \pi R_0^2 \quad (5)$$

where  $h_I$  is the clearance height at the inlet and  $h_e$  is the clearance height at the exit, with  $R_0$  the rotor radius. Tolerance buildup in both the hardware and the data are such that Eq. (5) cannot be ruled out even though Eq. (4) will be used herein.

#### RESULTS AND DISCUSSION

In this section we will first discuss the flow data simulation of normal operations (concentric) and then the abnormal- to the point of rub-case (fully eccentric) for a seal with various convergent tapers. The nominal tapers  $0.0^\circ$ ,  $0.2^\circ$ ,  $0.3^\circ$ ,  $0.4^\circ$  will be used to characterize the respective geometries. In all cases, ambient gases will be used and data taken with back-pressure varied from 0.25 to 1.4 MPa. For specifics on the geometries, consult Table 1, and note that the normalizing area  $\bar{A}$ , given by Eq. (4) is used throughout.

##### Concentric Geometry

For the  $0.0^\circ$ ,  $0.2^\circ$ ,  $0.3^\circ$ ,  $0.4^\circ$  taper configurations reduced mass flux data for fluid nitrogen are shown as a function of reduced pressure in Fig. 6 along with some unpublished data for the Shuttle seal 1 (unmodified version of Fig. 4). In general the results are monotone with a few questionable points at high flow rates, which are really at the limit of the facility.

Figure 7 represents a similar plot for gaseous hydrogen, except that, due to time schedules, no hydrogen data were taken with the  $0.2^\circ$  taper geometry.

##### Fully Eccentric Geometry

The fully eccentric case represents a near-rub and a complex inlet geometry subject to separation effects not usually considered in flow dynamics (2-4). More will be said about this problem later.

Figure 8 represents the reduced mass flux results for the  $0.0^\circ$ ,  $0.2^\circ$ ,  $0.3^\circ$  taper fully eccentric configurations using fluid nitrogen. Also plotted are some unpublished Shuttle seal 1 results and the locus of representing the concentric position data. The flow rates are higher than the concentric position by perhaps 6 percent and complex pressure profile behavior was noted. The reason may be geometric as strongly suggested from both the nitrogen and hydrogen data; however, at this time it remains unresolved.

Figure 9 is a similar plot for fluid hydrogen with a limited number of Shuttle seal 1 points and the locus of representing concentric position data is for comparison. No hydrogen data were taken for the  $0.2^\circ$  taper geometry and due to finding of some uncharacteristic and unresolved pressure profile results, the  $0.4^\circ$  fully eccentric taper was not machined.

#### Normalizing Constant C

To determine the constant C of Eq. (2), all the data were normalized using  $n = 1/2$  and  $m = 1$ , and the resulting value of C was plotted as a function of reduced pressure  $P_{R0}$  as Figs. 10 and 11. For the nitrogen and hydrogen data there does appear to be a trend with  $P_0$  and  $m \sim 1.02$  per theory, however the trend is weak and inconclusive. Further,  $n = 0.5$  does appear to group these data better than  $n = 0.55$ , and as noted earlier, some improvement can be made over a limited range with a specific fluid by changing the exponents. The nominal values C for these data are:

$$C = 0.153 \quad \text{concentric}$$

$$C = 0.158 \quad \text{fully eccentric}$$

This is in reasonable agreement with the theory considering a  $0.2 P_0$  pressure loss at the inlet. Under such conditions the constant should be  $C = 0.16$ .

#### Other Factors

The pressure profiles represent a significant effort, however as noted, the results are complex. First the number of pressure taps are simply not sufficient to establish the profiles either axially or circumferentially. Consequently, the pressure profile results are of marginal value but several indicative results should be noted for the fully eccentric configurations:

ORIGINAL PAGE IS  
OF POOR QUALITY



1. The overall stiffness of the conical seal configuration, as simulated, appears to be less than or equal to the straight seal ( $0.0^\circ$  taper) configuration.

2. It appears that the axial pressure profile for the  $0.0^\circ$  taper separates within the passage with a subsequent crossover from positive to negative stiffness. In all cases it appears that the total stiffness is still positive, but one must recall that these are static tests and such behavior can effect shaft instabilities under dynamic conditions.

3. It appears that a "shock" can develop within the seal with the largest effect noted in the straight seal. The pressure profiles, the nature of the "shock" and associated separation requires further investigation.

#### SUMMARY

The homogeneous equilibrium choked flow analysis and the principle of corresponding states have been extended to the choked flow of gases through static configurations which simulate dynamic seal behavior under high pressure gradients with the following results:

1. The reduced flow rate for gaseous nitrogen or hydrogen flowing through convergent conical or parallel passage geometries can be adequately represented by Eq. (2) with  $m = 1.0$  and  $n = 0.5$ . It can be inferred using the extended theory of corresponding states that any simple gas or mixtures of simple gases will also follow this formula.

2. For equilibrium nozzle computations,  $C = 1/5$ . Therefore assuming a  $0.2 P_0$  flow loss at the sharp edge the constant (C) would be 0.16. The data indicate (for  $n = 0.5$  and  $m = 1.0$ ):

$$C = 0.153 \quad \text{concentric}$$

$$C = 0.158 \quad \text{fully eccentric}$$

These constants may converge if the minimum stagnation choking pressures were accurately known for each configuration.

3. The pressure profiles within these configurations are complex and separation (shock) effects a change from positive to negative stiffness within the simulated seal however the overall stiffness appears to be positive.

4. Assessment of pressure profiles simulating dynamics requires multi-axial and circumferential pressure taps; further work is required here.

## REFERENCES

1. Fleming, David P.: High Stiffness Seals for Rotor Critical Speed Control. NASA TM X-73654, 1977 (ASME Paper 77-DET-10).
2. Hendricks, R. C.: Some Aspects of a Free Jet Phenomena to 105 L/D in a Constant Area Duct. Paper B1-78 XV Congress of Refrigeration, Venice, Italy, 23-29 Sept. 1979.
3. Hendricks, R. C. and Poolos, N. P.: Critical Mass Flux Through Short Borda Type Inlets of Various Cross Sections. Paper B1-77 XV Congress of Refrigeration, Venice, Italy, 23-29 Sept. 1979.
4. Hendricks, R. C.: A Free Jet Phenomena in a 90°-Sharp Edge Inlet Geometry. Paper Submitted to Cryogenic Engr. Conf. U. of Wisconsin, Madison, 21-24 Aug. 1979.
5. Hendricks, R. C.; Graham, R. W.; Hsu, Y. Y.; and Friedman, R.: Experimental Heat Transfer Results for Cryogenic Hydrogen Flowing in Tubes at Subcritical and Supercritical Pressures to 800 Pounds Per Square Inch Absolute. NASA TN D-3095, 1966.
6. Hendricks, R. C.; Simoneau, R. J.; and Barrows, R. F.: Two-Phase Choked Flow of Subcooled Oxygen and Nitrogen. NASA TN D-8149, Feb. 1976.
7. Hendricks, R. C. and Simoneau, R. J.: Application of the Principle of Corresponding States to Two-Phased Choked Flow. Presented at the 74th National AIChE Meeting, New Orleans, March 1973, NASA TM X-68193.
8. Hendricks, R. C. and Simoneau, R. J.: Two-Phase Choked Flow in Tubes with Very Large L/D. Advances in Cryogenic Engineering, Vol. 23, 1977, pp. 265-275.
9. Simoneau, R. J. and Hendricks, R. C.: Generalized Charts for Computation of Two-Phase Choked Flow of Simple Cryogenic Liquids, CRYOGENICS, Vol. 17, Feb. 1977, pp. 73-76.
10. Hendricks, R. C.: Normalizing Parameters for the Critical Flow Rate of Simple Fluids Through Nozzles. Proc. of the Fifth International Cryogenic Engineering Conf. (and Int. Inst. of Refrigeration), Kyoto, Japan, 1974.
11. Shapiro, A. H.: The Dynamics and Thermodynamics of Compressible Fluid Flows. Rolland Press.

TABLE 1. - GEOMETRIC PARAMETERS

Concentric				
Diameter centerbody, cm	Diameter Inlet, cm	Diameter Outlet, cm	Nominal taper, deg	$\bar{A}$
8.4244	8.4397	8.4397	0.0	0.2018
	8.4478	8.4401	.2	.2424
	8.4524		.3	.2625
	8.4587		.4	.2861
Fully eccentric				
8.4244	8.4409	8.4409	0.0	0.2178
	8.4486		.2	.2524
	8.4536		.3	.2749
Seal length = 1.232 cm				
Location of pressure taps 0.000 cm is at the seal inlet				
0°	90°	180°	270°	
P02 - 2.98 cm	-----	P06 - 2.98 cm	-----	
P05 - 0.60	-----	P09 - 0.05	-----	
P1 0.051	-----	P5 0.064	-----	
P2 0.660	P90 0.66	P6 0.66	P270 0.66	
P3 0.998	-----	P7 0.988	-----	
P4 1.295	-----	P8 1.295	-----	

TABLE 2. - FLOW NORMALIZING PARAMETERS

Fluid	$G^*$ g/cm <sup>2</sup> -s	$T_c$ , K	$P_c$ , MPa
Nitrogen	6010	126.3	3.417
Hydrogen	1158	33.	1.296
Oxygen	8670	154.78	5.082
Argon	9404	150.7	4.865
Methane	5094	190.77	4.627

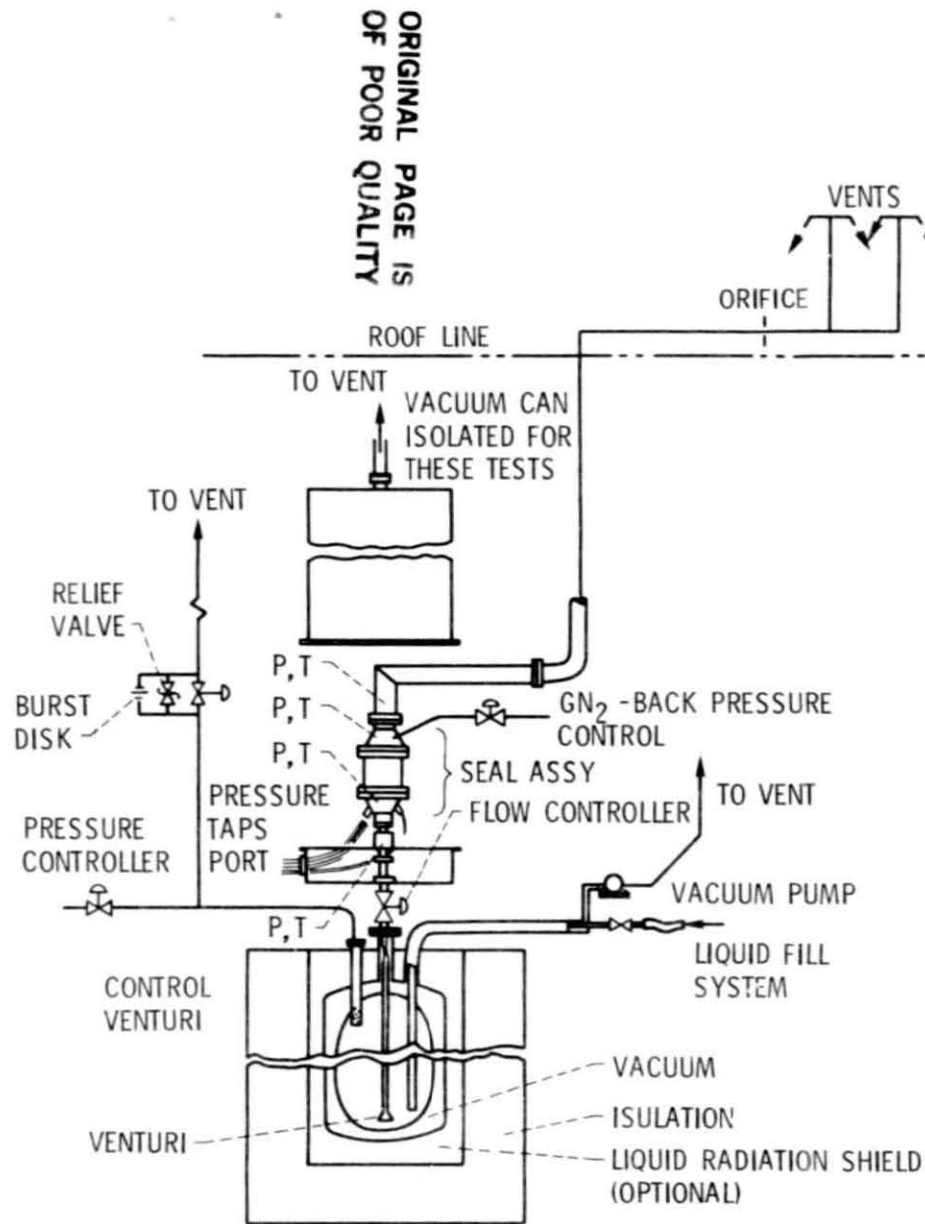


Figure 1. - Schematic of test installation.

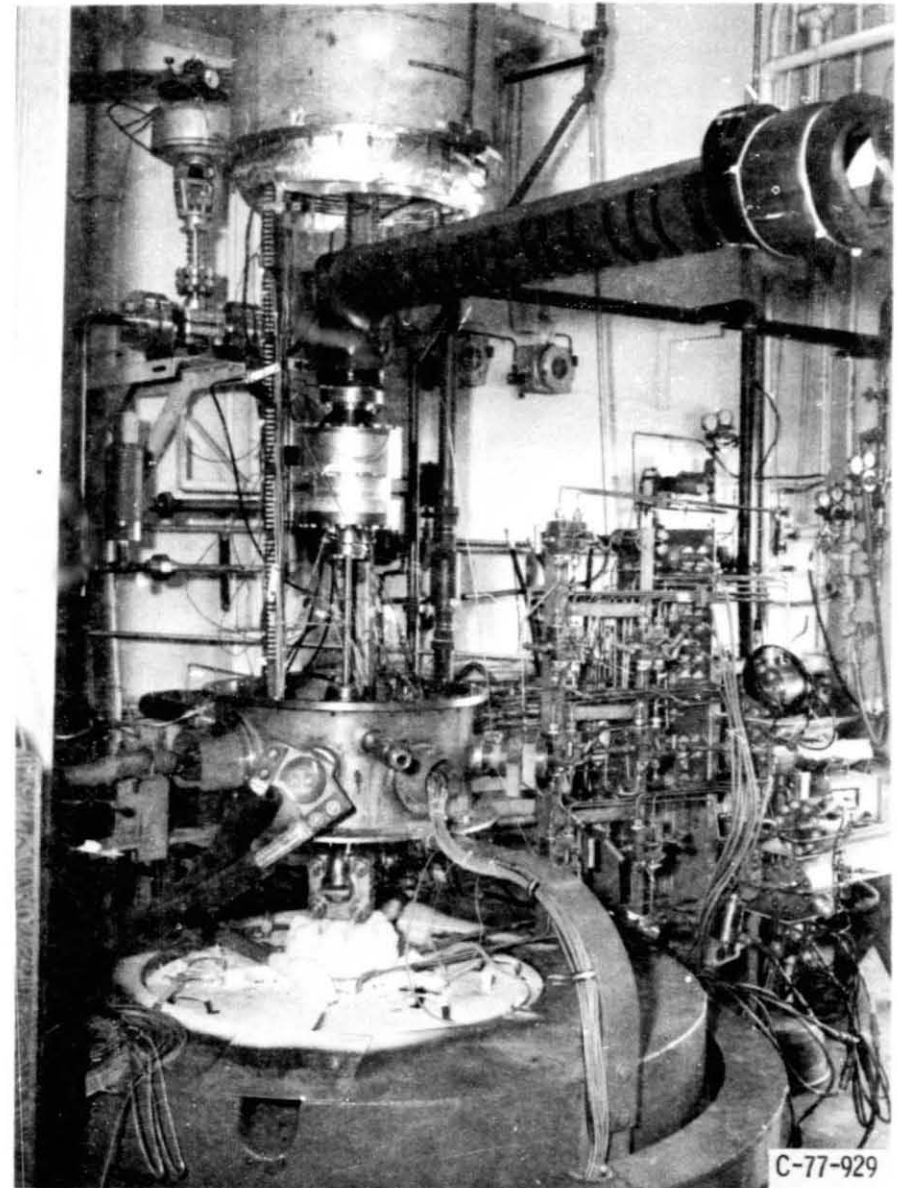


Figure 2. - Simulated seal assembly installation.

C-77-929

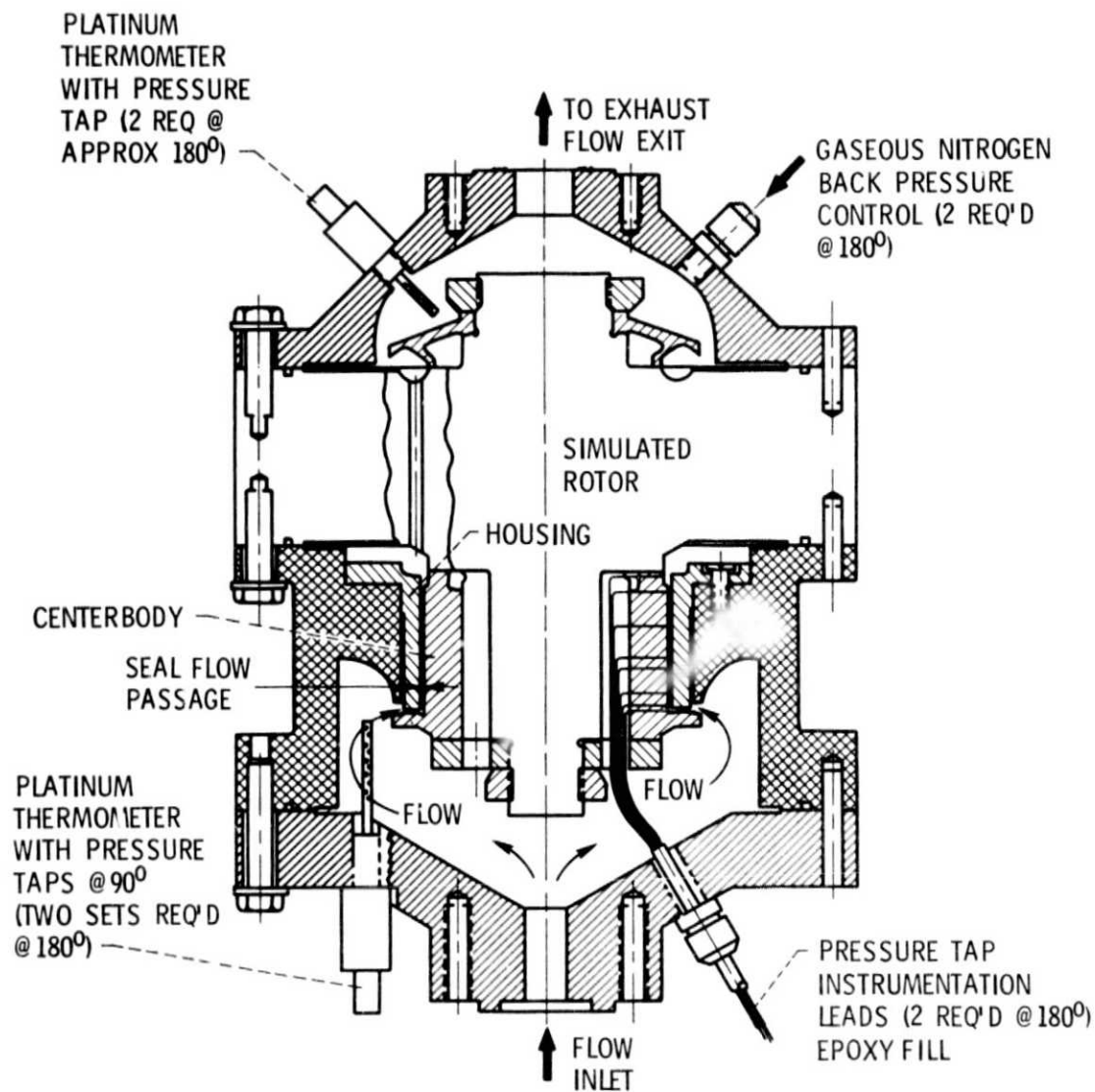
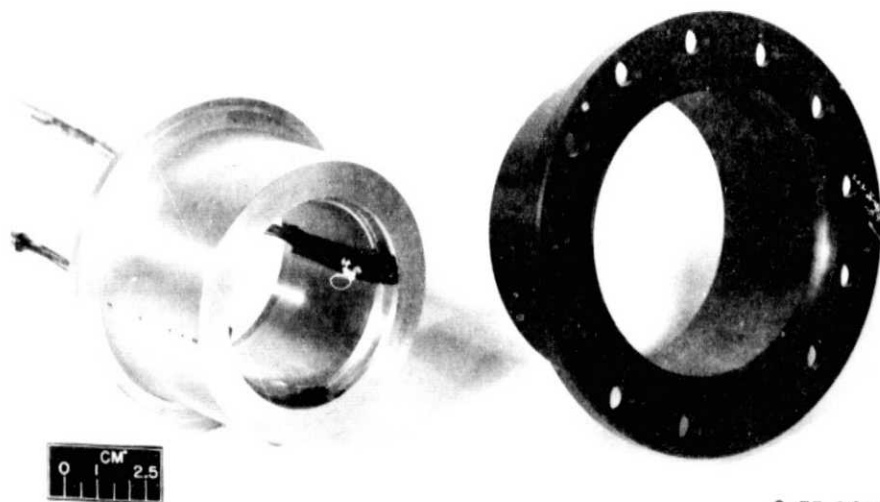
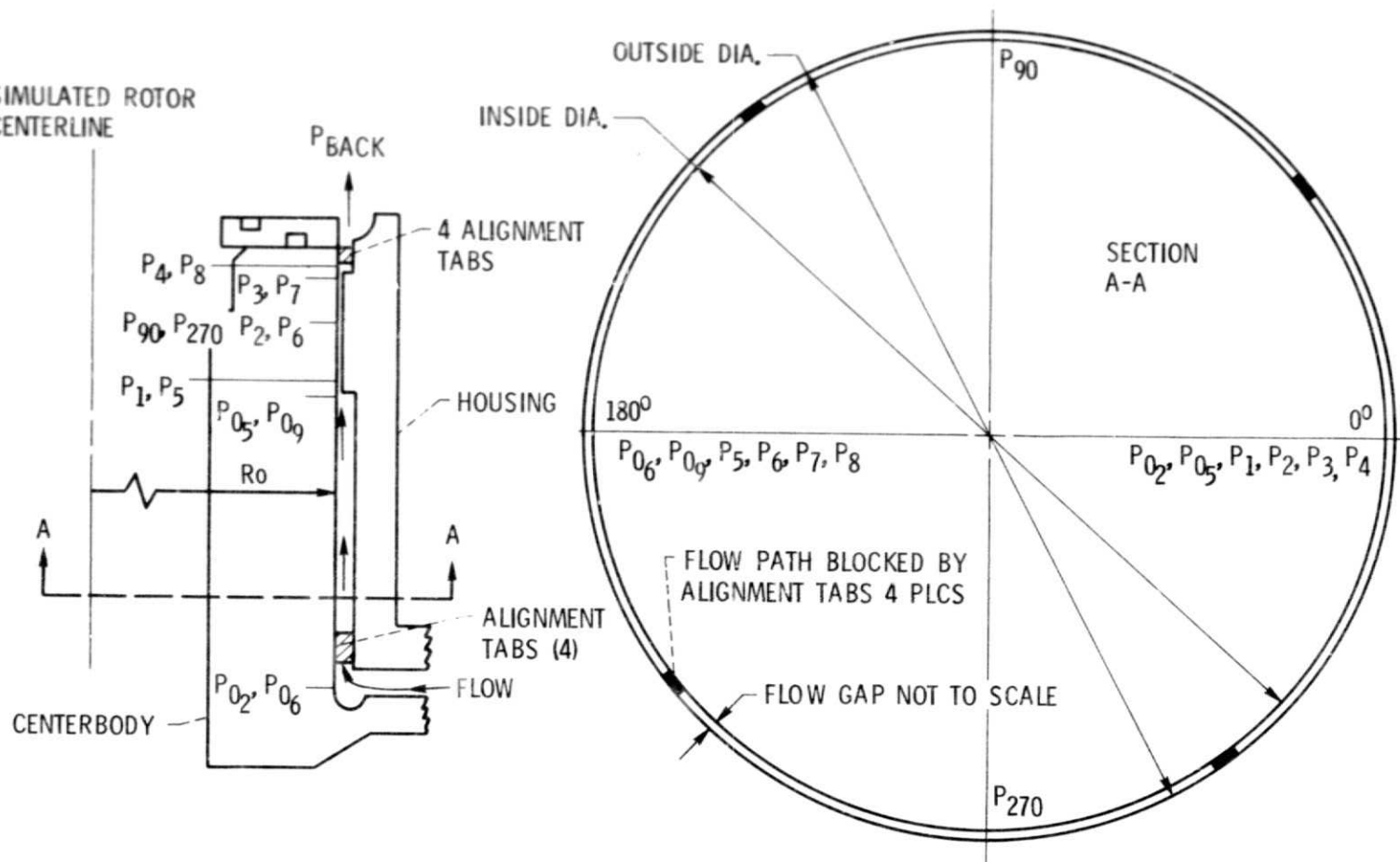


Figure 3. - Cross section view of simulated seal configuration.



C-77-1466

Figure 4. - Simulated shuttle seal No. 1, centerbody and housing with instrumentation.



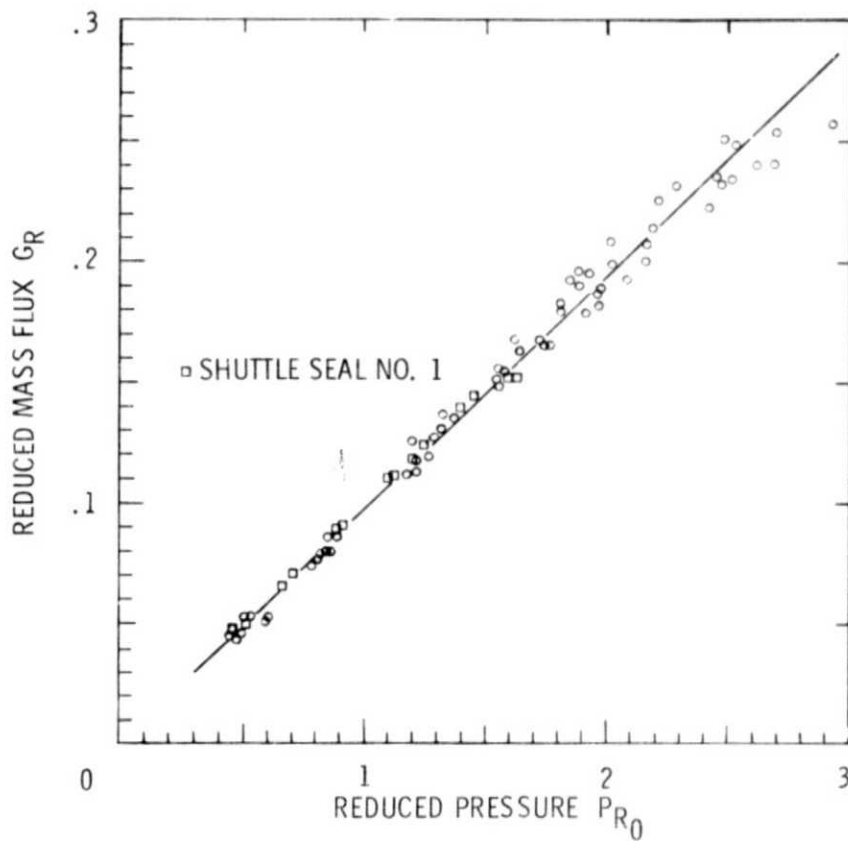


Figure 6. - Reduced mass flux as a function of reduced stagnation pressure for gaseous nitrogen flowing through the  $0.0^\circ$ ,  $0.2^\circ$ ,  $0.3^\circ$ ,  $0.4^\circ$  taper simulated seal configurations, concentric position.

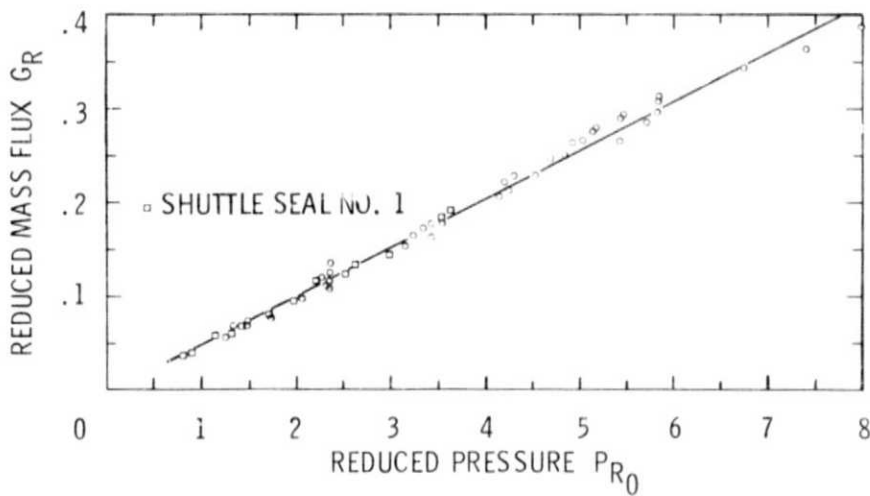


Figure 7. - Reduced mass flux as a function of reduced stagnation pressure for gaseous hydrogen flowing through the  $0.0^\circ$ ,  $0.3^\circ$ ,  $0.4^\circ$  taper simulated seal configurations, concentric position.



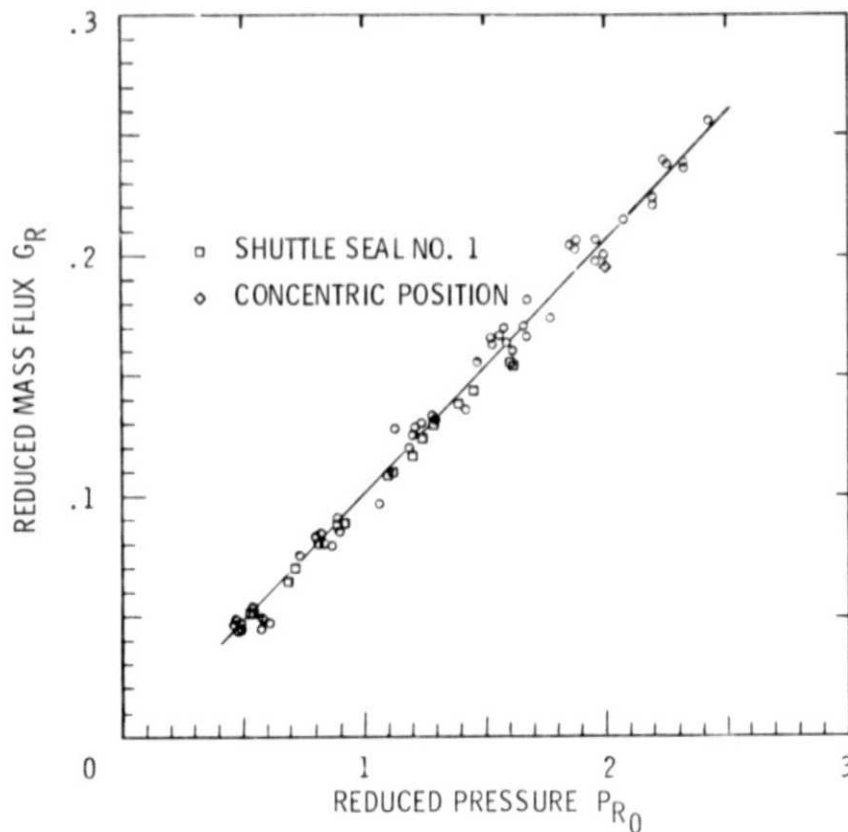


Figure 8. - Reduced mass flux as a function of reduced stagnation pressure for gaseous nitrogen flowing through the  $0.0^\circ$ ,  $0.2^\circ$ ,  $0.3^\circ$  taper simulated seal configurations, fully eccentric position.

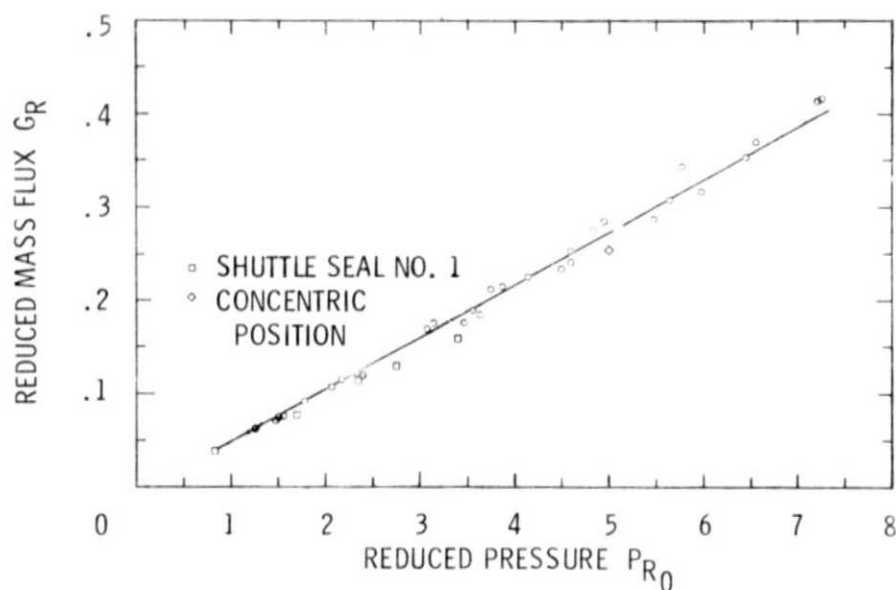


Figure 9. - Reduced mass flux as a function of reduced stagnation pressure for gaseous hydrogen flowing through the  $0.0^\circ$ ,  $0.3^\circ$  taper simulated seal configurations, fully eccentric position.

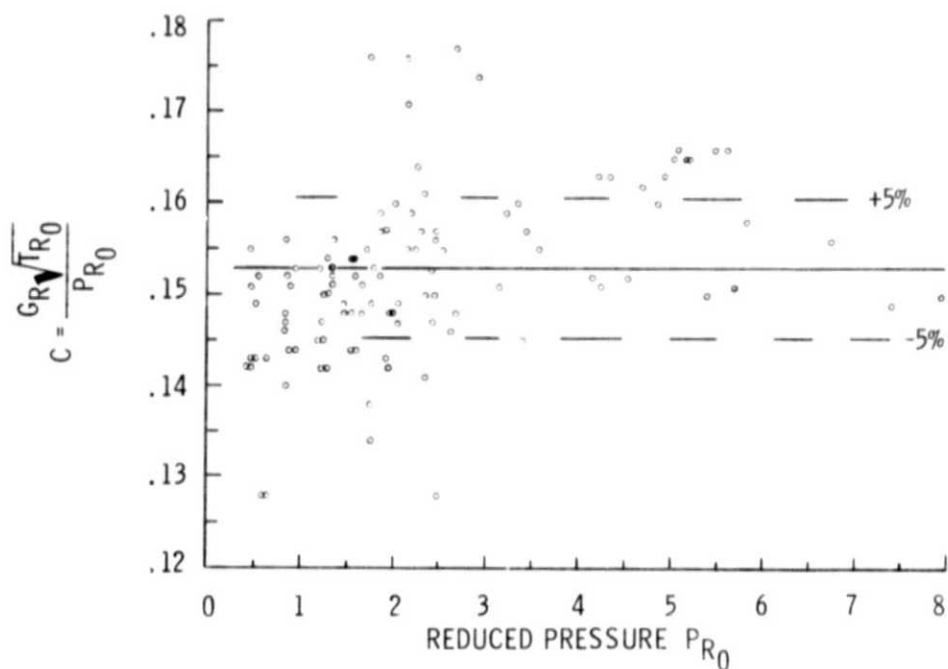


Figure 10. - Distribution of  $C$  with reduced pressure for gaseous nitrogen or hydrogen flowing through simulated seal configurations with and without convergent taper, concentric position.

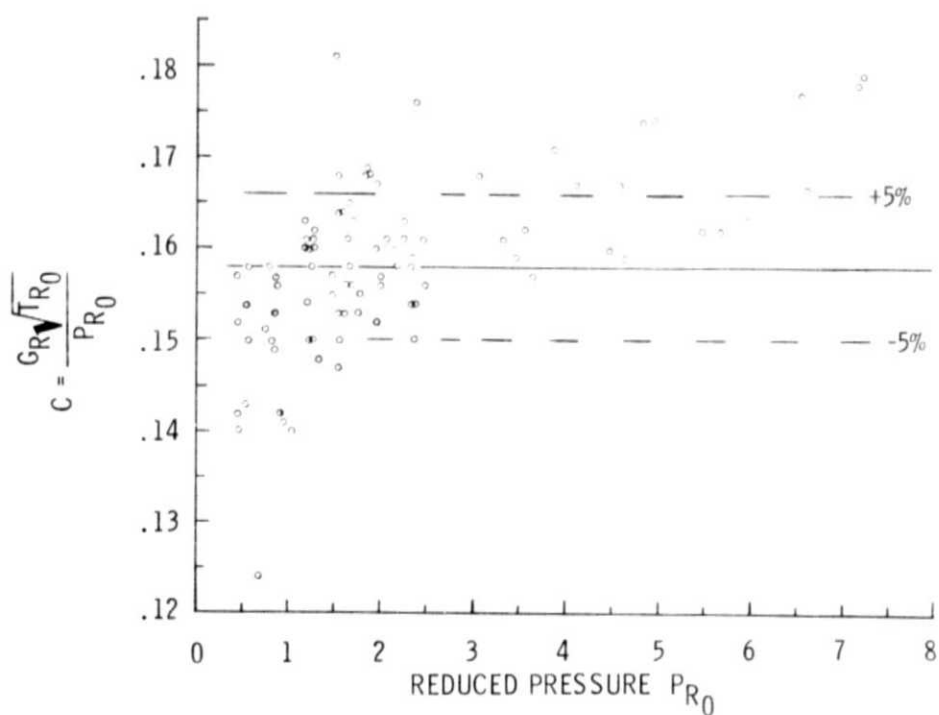


Figure 11. - Distribution of  $C$  with reduced pressure for gaseous nitrogen or hydrogen flowing through simulated seal configurations with and without convergent taper, fully eccentric position.